

IMPROVED MICROSTRUCTURE BY OPTIMIZED WATER REQUIREMENTS

M. Hunger (1), H.J.H. Brouwers (1)

(1) Department of Construction Management & Engineering, Faculty of Engineering Technology, University of Twente, The Netherlands

Abstract

In everyday construction practice concrete is often produced applying water amounts in excess of what intrinsically is needed for appropriate workability and complete hydration. This is especially true for high slump and self-compacting concretes (SCC). For an increased robustness of concrete to water overdose the building chemistry sector supplies viscosity modifying admixtures (VMA), which would not have been needed when the amount of mixing water was optimized beforehand.

Therefore, in this research the spread-flow test has been analyzed in more detail. In this way new measures are derived which contribute to a deeper understanding of wet granular mixtures at the onset of flowing. The deformation coefficient which is derived by the spread-flow test was confirmed to correlate with the product of Blaine surface and intrinsic density of the individual powders when the mixture is flowing only under its own weight. Similarly, correlations with equal accuracy have been found with a computed specific surface based on measured particle size distributions instead of the Blaine surface. Using simple flow experiments it was furthermore possible to derive an overall factor for assessing the non-spherical shape of the powder particles. A good correlation of this computation algorithm was derived compared to the standard Blaine method.

Finally, a constant water layer thickness around the powder particles was derived for all powders at the onset of flowing. This implies the possibility to predict flow behavior of mortar and concrete mixtures only based on the knowledge of their granular characteristics. This water layer thickness is of different nature and size as the well-known ITZ.

1. INTRODUCTION

The durability of concrete cannot be characterized with a uniform value. But the impermeability of concrete against water and deleterious matters dissolved or suspended in water is always one of the most crucial aspects. For this reason the minimization of the fraction of capillary pores is of vital importance for the impermeability and durability of concrete [1].

The percentage of capillary pores is basically a result of the w/c ratio, degree of hydration and the type of cement. Though the total amount of mixing water is limited by w/c ratios, the amount of water solely needed for workability reasons is often exceeded. This is especially the case when dealing with SCC. Here, water in excess of the intrinsically needed amount of lubricant is handled with VMAs. In other words the inadequate knowledge of water demands sufficient for flowing is one of the main reasons for the application of VMAs which do not serve for another purpose. This excess water is producing additional capillary pores which weaken the durability of the microstructure. Already Popovics [2] remarks how little work has been done to express numerically the influence of the granular composition of concrete on its water demand, considering the overwhelming significance of the quantity of mixing water on the overall quality of concrete, and in particular on the microstructure.

In this respect two issues have to be considered. These are (i) the optimization of all solids regarding their particle size distribution, and (ii) the knowledge of the optimum water demand or the amount of water at the onset of flowing. The former issue results in a dense microstructure with less void fraction to be filled with water and air, whereas the latter prevents the introduction of water in excess of the required amounts.

The water demand of powders, the finest particles in concrete, is a significant parameter for the design of concrete. It is composed of a layer of adsorbed water molecules around the particles and an additional amount needed to fill the intergranular voids of the powder system. Since powders provide by far the biggest part of the total specific surface area, they have the strongest influence on the total water demand of a concrete mix. Consequently, they should have a preferably low water demand. The spread-flow test is, amongst others, a suitable test procedure for the determination of water demands of powders, mortars and even complete concrete mixtures.

Literature [3] shows that the execution of spread-flow tests is not only limited to water/powder ratios indicating the onset of flowing. However, this test in addition provides more information on the relation of water demand sufficient for flowing, void fraction, and the influence of specific surface area on the variation of fluidity. In this regard Brouwers and Radix [3] found a linear dependence of specific surface area and relative slump when sufficient water is present for flow. This hypothesis is going to be addressed in the following.

2. FLOW EXPERIMENTS

The spread-flow test (or sometimes referred to as paste line test or mini-slump flow test) according to Okamura and Ozawa [4] appears to be the classical method for the determination of the water demand of powder materials involved in SCC. Thereby suspensions are produced being composed of the powder to be analyzed and varying quantities of water. After appropriate mixing following a defined mix regime, the suspension is filled in a special conical mold, the Hägermann cone, which is lifted in order to allow free flow for the paste without any jolting. From the spread-flow of the paste, two diameters perpendicular to each other (d_1 and d_2) can be determined. Their mean is deployed to compute the relative slump (Γ_p) via:

$$\Gamma_p = \left(\frac{d}{d_0} \right)^2 - 1 \quad \text{with } d = \frac{d_1 + d_2}{2} \quad (1)$$

where d_0 represents the base diameter of the used cone, 100 mm in case of the Hägermann cone. The relative slump Γ_p is a measure for the deformability of the mixture, which was originally introduced by Okamura and Ozawa [4] as relative flow area R.

In order to satisfy statistical needs at least four different water/powder-ratios have to be tested to obtain a reliable trend line. Thereby, every single water/powder-ratios is represented by a freshly prepared mix and explicitly not by adding water to the present mix. It is furthermore recommended [5] to aim on spread-flows of 140 mm up to 230 mm, which corresponds to a relative slump Γ_p of 0.96 to 4.29 using the Hägermann cone. Other literature [6] refers to a range from 0.2 to 15. It is believed that any spread-flow can be accepted for assessment, as long as it shows a measurable and symmetrical spread, and possesses no signs of segregation (obvious centric pile) or bleeding (corona of bleeding water).

Now all measured Γ_p (cp. Figure 1) are plotted versus their respective water/powder volume ratios (V_w/V_p) involving the respective specific densities of the deployed materials. A straight line is fitted through the derived data points afterwards. The intersection of this linear function with the axis of ordinates at $\Gamma_p = 0$ depicts the retained water ratio where no slump takes place [7]. In other words, this denotes the maximum amount of water which can be retained by the particles. Any water in excess will turn the wet particle mix into a concentrated suspension. This point is referred to as water demand or retained water ratio, which is known as β_p in concrete technology.

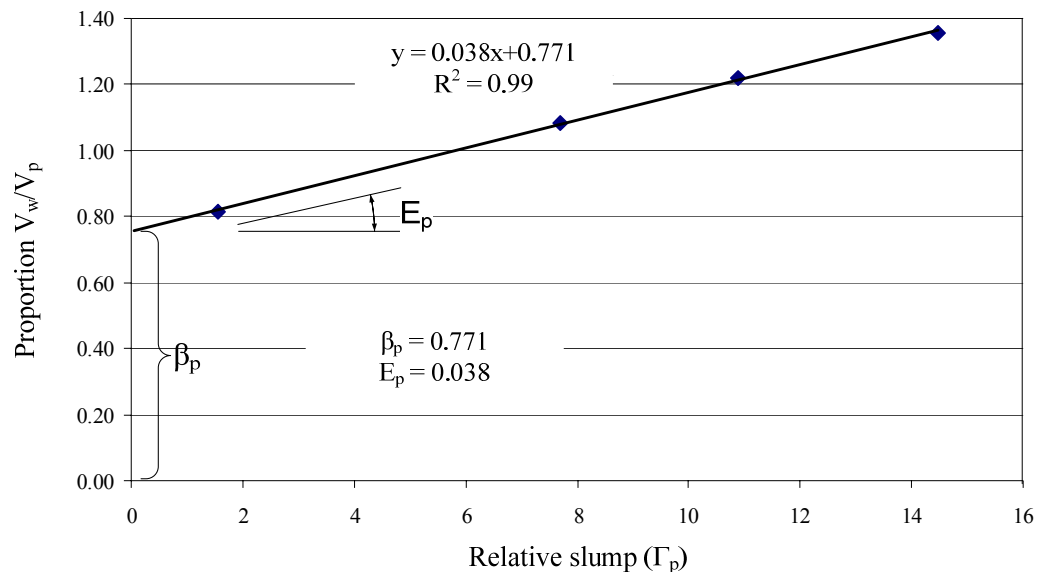


Figure 1: Analysis of a spread-flow experiment

From this analysis a linear relation can be derived for each material. The outcome of this linear regression is a function of the type:

$$\frac{V_w}{V_p} = E_p \Gamma_p + \beta_p \quad (2)$$

In addition to the water demand β_p , information is also gained with the value E_p , which is the slope of the function. This is the so-called deformation coefficient which can be understood as a measure of sensitivity on the water need for a specified flowability. Therefore, materials having a lower E_p , i.e. showing flat slopes, respond with more pronounced change in deformability to a certain change in water dosage than materials having a steeper slope. Thus small changes in the water content have a stronger influence on the relative slump. This way, materials can be identified that tend to bleed or segregate more easily than other powder materials in mortars and concrete mixes.

3. ANALYSIS OF FLOW EXPERIMENTS

3.1 Derivation of a shape factor

When computing water demands based on surface area, one should consider the particles' shape. This mostly deviates from ideal sphere shape and therewith increases specific surface and hence the water demand. In the following the derivation of a shape factor, based on flow experiments with water-powder mixtures, is described. This procedure will indirectly provide a shape factor, not being based on direct measurements of particle dimensions, but relevant for water-powder flow.

The particle shape factor is expressing the ratio of an effective particle surface area of an irregularly formed particle to the surface area of an ideal sphere with equal volume. According to this definition, the ideal, smooth sphere would have a shape factor, ξ , of 1. This represents a three-dimensional approach, being based on volume considerations. In principle two approaches are reported in literature. On the one hand two-dimensional particle shape measurements are conducted with the help of images or projections. On the other hand three-dimensional analysis with individual particles is carried out by measuring the principal axes of an irregularly shaped particle. Both approaches are direct measurements as specific geometrical characteristics of a particle are considered.

Besides the classical approach of directly measuring particle dimensions there are also indirect ways to derive an overall shape factor. The above described methods provide a number of measures, which can describe particles in detail. However, their combination to an overall-shape factor turned out to be difficult. Motivated by the varied usage of shape factors, there is an interest to find suitable values with more general measurement techniques or in other words to find correlations with values measured anyway. One approach was for example given by Reschke [8], who is forming a ratio of the directly measured Blaine surface a_{Blaine} and the computed surface area, a , via:

$$\xi_{\text{Reschke}} = \frac{a_{\text{Blaine}}}{a} \quad (3)$$

The surface area, a , is a computed measure derived from the particle size distribution and assuming spheres with equivalent diameter. So, Reschke [8] used Blaine values to calibrate and derive shape factors. Therefore, the obtained shape factors still contain the systematical error which is involved in a Blaine measurement. Subsequent to the computation Reschke verified the plausibility of the derived shape factors by means of a SEM-documentation of selected powder materials. Both, computed shape factors as well as the visual impression of the micrographs are in good agreement. Groups of similar materials are formed when

organizing this computed shape factors in ascending order, i.e. each material type is forming an own narrow range of shape factors.

In total Reschke determines a range of shape factors $\xi_{Reschke}$ from 1.00 up to 3.08, of which 1.00 represents micro-glass spheres and 3.08 a kaolin type. However, the value for the micro-glass spheres was not measured but assumed to be unity. Therefore this model cannot be considered to be aligned with the ideal model case. Summarizing, this model gives plausible results being in line with the SEM-image analysis.

For the first instance the particle shape data provided by Reschke [8] is used to correct the computed surface area of the present analysis for their non-spherical particle shape. In the following, a model for the computation of shape factors will be derived based on flow experiments. Later, these values will be compared with the shape factors derived by Reschke. In Table 1 the selected shape factors are given in combination with the sphere-based surface area, as well as with the shape corrected surface area.

Table 1: Surface area properties of the powders

Material	Specific surface area				
	Blaine a_{Blaine} [cm ² /g]	Computed sphere based S_{sph} [cm ² /cm ³]	Shape factor		Computed Non-spherical S [cm ² /cm ³]
			$\xi_{Reschke}$	Computed ξ	
CEM I 52.5 R - micro cement	-	26,624	1.68	1.73	44,728
CEM I 52.5 N	-	15,749	1.68	1.57	26,458
CEM I 32.5 R	-	12,367	1.52	1.62	18,798
CEM III/B 42.5 N A	4,830	12,687	1.58	2.03	20,045
CEM III/B 42.5 N B	4,500	17,775	1.58	1.36	28,085
Limestone powder	4,040	13,850	1.26	1.22	17,451
Granite powder	-	13,051	1.50	1.26	19,577
Marble powder A	4,580	14,739	1.50	1.16	22,109
Marble powder B	-	12,573	1.50	1.87	18,860
Marble powder C	-	13,391	1.50	1.29	20,087
Fly ash A	2,840	13,113	1.20	1.00	15,736
Fly ash B	-	13,419	1.20	1.09	16,103
Gypsum A	-	7,970	1.80	1.30	14,346
Gypsum B	-	9,713	1.80	1.18	17,483
Trass	-	15,603	1.20	1.10	18,724

One of the major hypotheses put forward by Brouwers and Radix [3] was that the relative slump of a water-powder mixture becomes a function of the specific surface area when

sufficient water is present for flow, i.e. $V_w/V_p > \beta_p$. This hypothesis was validated by relating the slope of the spread-flow function E_p (cp. Eq. (2)), the deformation coefficient, to the specific surface area S . The specific surface area was taken from Blaine (a_{Blaine}) multiplied with the specific particle density ρ_s to obtain the specific area per volume of powder. From the observations it was concluded that the larger the internal surface, the larger the deformation coefficient (the more water is required to attain a certain relative slump). Accordingly, the following linear relation was derived:

$$E_p = \delta \cdot a_{Blaine} \cdot \rho_s = \delta \cdot S \quad (4)$$

with δ representing the thickness of an idealized water layer, surrounding the particles of a water-powder suspension with $V_w/V_p = \beta_p$, i.e. the onset of flowing. Brouwers and Radix [3] found a mean δ of 41.32 nm. This range is also confirmed by Marquardt [9], who found a layer thickness of about 150 water molecules for the water demand of particle fractions by means of sorption experiments. This layer thickness corresponds to approximately 45 nm as the size of one water molecule is about 3 Å.

In the following section the above approach is applied for the derivation of a shape factor, considering a larger number of powder samples. A further modification is introduced by using the uncorrected (so assuming spheres), computed specific surface area a_{sph} instead of the Blaine surface area. This PSD-based computed surface area is a weight-based measure like the Blaine surface. It is chosen as the Blaine measurement holds some uncertainty in itself, especially for powders of high fineness, since the underlying Carman-Kozeny equation, used in this air permeability method, is not valid for particles smaller than 10 μm (Hunt [10]). In principle the computational models for laser diffraction and the measurement itself also contain some inaccuracy, but no systematical error is additionally introduced, as in the case by using Blaine measurements. As the derived shape factor will later be applied on the detailed PSD with the same systematical error, there will not be a multiplied effect on the corrected computed surface area. Furthermore, the PSD data is available and Blaine does not need to be determined in addition. Blaine-test and computed surface area both describe the outer surface of particles and apart from a systematic deviation due to different measurement principles they provide basically the same information. This is confirmed by Robens [11] as well.

Now, plotting the computed specific surface area (S_{sph}) of these powders versus the deformation coefficient E_p , (Fig. 2) is obtained. Figure 2 provides the necessary results of the spread-flow tests on these powder materials. Note that E_p , β_p and S_{sph} used in this graph are all volume based, and S_{sph} is the specific surface if the particles would be truly spherical. With the help of linear regression a relation was derived for these measures. Based on the assumption that the slope of a paste line becomes a function of SSA when $V_w/V_p > \beta_p$ is satisfied, the regression line has to intercept the point $E_p = 0$. Now, assuming straight lines from every data point through the origin would result in lowest slopes for the two fly ash powders involved, the two materials with the most spherical shape. Their true surface will namely be closest to the actual one, as they are close to spherical shape. As the computation of SSA is based on the assumption of spheres, a shape factor larger than unity (i.e. $\xi > 1$) is necessary to correct for non-spherical shape, i.e. a positive displacement of all data points parallel to the axis of abscissa (increase of SSA). Hence, the material having the lowest slope (δ) could serve as model particle to calibrate the others. Finding the lowest slope for the

materials with the most sphere-like shape could already serve as a simple validation of the presented approach.

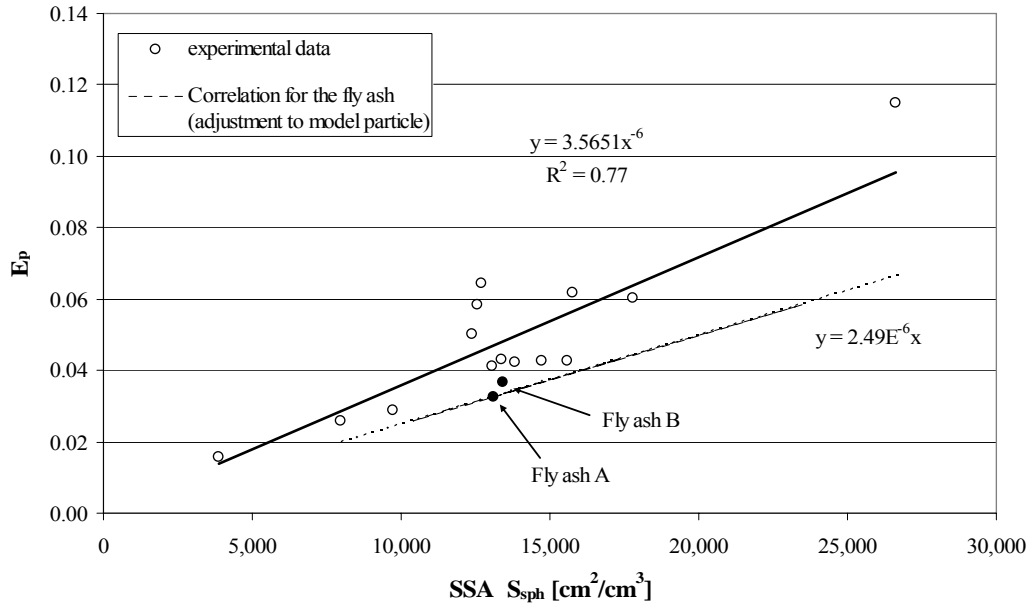


Figure 2: A Plot of uncorrected, computed and volume based specific surface area versus the respective deformation coefficient E_p derived from spread-flow tests

In order to further validate the proposed relation between S_{sph} and E_p , shape factors have been selected in a next step. This selection was based on the work of Reschke [8] and is not related to measured properties of the materials evaluated. In this way the different cement types were assigned with shape factors of equivalent cement types from Reschke's research, e.g. a limestone powder was specified with the averaged shape factor for limestone powders taken from Reschke. These selected shape factors are given in Table 1. It should be understood that they will only serve as a first comparison. Plotting these newly derived and now shape-corrected SSAs against E_p results in an improved coefficient of determination.

Based on these considerations a particle shape factor ξ was derived to correct all available and only sphere-based SSA in such a way that they fit on the regression line given by the particles that come closest to spherical shape (i.e. $\xi = 1$), which in this case is fly ash (cp. Fig. 2). The equation based on the fly ash then reads as:

$$E_p = \delta \cdot a \cdot \rho_s = 2.49 \cdot 10^{-6} \text{ cm} \cdot S, \quad \text{with } \delta = 2.49 \cdot 10^{-6} \text{ cm} \quad (5)$$

Now, substituting E_p with the associated deformation coefficients determined by the spread-flow experiments and assuming a film thickness of 24.9 nm, for every material, a theoretical specific surface area S is computed. Comparing this theoretical surface with the uncorrected surface S_{sph} , with ξ set equal to unity, a new shape correction factor ξ can be derived. This factor reads as:

$$\xi = \frac{S}{S_{\text{sph}}} \quad (6)$$

Applying Eq. (6), shape factors have been computed for all given materials. These factors can be found in Table 1. The corresponding shape factors, chosen on the basis of Reschke [6] are included in the same table as well. Comparing the data obtained, it can be noticed that derived shape factors correlate well with the ones based on Reschke. This further validates the approach followed here. In total the shape factors range from 1.00 for the fly ash (as imposed here) up to 2.03 for the CEM III/B 42.5 N, the latter appearing to have the biggest shape deviation from smooth spheres. Note that all shape factors are larger than unity indeed, which is consistent with the proposed approach. The second type of fly ash (fly ash B) yields a shape factor only slightly higher than fly ash A. Differences in fly ash shape factors, also notably higher ones, can be explained by the partly porous surface structure, fly ash can possess. The surface structure of fly ash is highly dependent on the formation conditions. Furthermore, fly ash also can contain other types of ashes, unburnt coke particles, quartz particles or broken hollow balls. However, the invoked spherical shape of fly ash, $\xi_{\text{FA}} = 1$, seems to be a good basis. Furthermore, if fly ash would turn out to have a shape factor slightly larger than unity, all shape factors derived here only need to be multiplied with this $\xi_{\text{FA}} > 1$.

3.2 Concept of constant water layer thickness

From Eq. (3) a value of 24.9 nm was derived for δ of fly ash, representing a constant water layer thickness. Note that this model is based on the computed specific surface area and calibration using fly ash particles as spherical model particles, and is confirmed by the results of other powders. Although this layer thickness is in a similar range like the one derived by Brouwers and Radix [3] being 41.32 nm, there is still a difference of about 40%, which is addressed here.

The Blaine surface as used by Brouwers and Radix [3], and the computed surface used in this study can explain the difference in derived film thickness. In the relevant literature most authors agree on linear correlation between Blaine fineness and the surface area calculated from PSD data. Robens et al. [11] found, for instance, a constant factor of 1.3 for the ratio of computed surface area to Blaine. Applying this factor on the data presented would increase the derived δ to 32.4 nm. For the readers interest it is noted, that this constant factor of 1.3, found by Robens et al. [11] is based on the automated surface computation of the deployed laser granulometer [12]. Its computation algorithm is based on a similar principle as the one applied in this study [13, 14]. However, there the geometric mean of a class is considered as mean diameter which results in larger surface areas compared to the arithmetic mean applied in this study [13]. The difference between both surfaces amounts to about 6% considering a size ratio of $u = 2$ (as being used in standard sieve sets). Furthermore, the underlying model particles are spheres as well. Therefore the surface area difference of 1.3 is based on the assumption of spheres. Considering the true surface of the angular materials, which were actually cements in the example of Robens et al. [11], would turn the deviation even bigger. Therefore, applying a shape factor in addition to the systematic deviation of Blaine surface and computed surface would result in an increased water layer thickness derived with the presented approach. Depending on the shape factors selected, it is a range of 42 nm to 48 nm when deploying the derived shape factors for blast furnace cements. This correlates with the film thicknesses found by Brouwers and Radix [3] who used Blaine values, and by Marquardt

[9]. High correlation between computed surface area and Blaine fineness was also found by Hunt [10], who derived a factor of 0.97. However, the two correlation factors from Robens et al. [11] and Hunt [10] cannot directly be compared since the latter based the surface area computation on cumulative mass distribution curves derived by sedimentation method. Furthermore, the addressed specific surface area calculation method is based on the assumption of spheres and deploys the arithmetic mean as characteristic diameter. A linear relation of computed specific surface area and measured Blaine surface is manifold confirmed in literature. Varying measurement techniques and different theoretical models, however, make their comparison difficult.

An analysis in this respect for the involved powders resulted indeed in a linear correlation, but with a higher factor. For a number of powders the Blaine value was determined and multiplied with the respective specific density. These values have been plotted versus the computed SSA, now shape-corrected by the addressed model. By means of linear regression a correlation factor of 1.67 was found (i.e. $a = 1.67a_{\text{Blaine}}$), so that:

$$S = 1.67 \cdot a_{\text{Blaine}} \cdot \rho_s \quad (7)$$

This increased ratio is explained by the shape correction, which now is included in this consideration. Taken the water layer thickness $\delta = 41.32$ nm from [3] again, which is based on Blaine, and using the derived factor between the surfaces, results in $\delta = 24.7$ nm as well. This should be understood as a correction of the systematic error of Blaine and the sphere assumption of the surface computation models. Hence, both derived water films, $\delta = 41.32$ nm in Brouwers and Radix [3] as well as $\delta = 24.9$ nm with the presented study, are in agreement with each other.

4. CONCLUSION

The present work addresses the spread-flow test or also referred to as mini-slump test. It is demonstrated that, based on simple flow experiments, a shape factor can be derived, which is needed to correct a computed specific surface area, derived from PSD data. This approach is new and shows an interesting alternative to the existing, extensively device-related direct measurement principles. Besides the approach introduced by Reschke [8], this is to the author's knowledge the first technique using sound standard measurements for the derivation of a shape factor, which considers form, angularity and surface structure of powder materials.

Furthermore, it gives new significance to the spread-flow test. In this regard the hypothesis proposed by Brouwers and Radix [3] is confirmed. According to them the relative slump of a paste becomes a function of the SSA when sufficient water is present for flow.

In this article a water layer thickness of about 25 nm is found for water/powder mixtures on the onset of flowing, i.e. having water contents of $V_w/V_p = \beta_p$. This obtained value corresponds with the figure found by [3]. Different correlations of e.g. Blaine surface and computed SSA have been found in literature, and also proven by own experiments (Eq. (7)). The factor 1.67, found here, explains the difference in the water layers, but in more general it expresses the difference between true surface and Blaine. Since the Blaine test is a simple and widely-used measurement, the derived correlation can be used to translate Blaine figures into computed figures based on PSDs (or backwards), which appears to result in information of equivalent or better accuracy. Furthermore, also fine particles, not being suitable for Blaine measurement can be expressed as "Blaine values".

The difficulty of predicting water requirements of concretes lies in the large number of variables involved, which of the particle shape is one of the most difficult to characterize [2]. Shape factor and the lubricating ability of the particle surrounding water layers are important characteristics for the prediction of water demands. The above approach should serve as a basis for a model including all pertinent factors regarding water requirement of concrete mixtures. This approach is based on the knowledge of granular properties and does not require time consuming trial tests anymore. This way a reliable prediction of mixing water requirements should be possible resulting in more dense and durable microstructure.

ACKNOWLEDGEMENTS

The authors wish to express their sincere thanks to the European Commission (I-Stone Project, Proposal No. 515762-2) and the following sponsors of the research group: Bouwdienst Rijkswaterstaat, Rokramix, Betoncentrale Twenthe, Betonmortelcentrale Flevoland, Graniet-Import Benelux, Kijlstra Beton, Struyk Verwo Groep, Hülskens, Insulinde, Dusseldorp Groep, Eerland Recycling, Enci, Provincie Overijssel, Rijkswaterstaat Directie Zeeland, A&G Maasvlakte, BTE and Alvon Bouwsystemen (chronological order of joining).

REFERENCES

- [1] Stark, J., Wicht, B. 'Dauerhaftigkeit von Beton – Der Baustoff als Werkstoff', Basel, Boston, Berlin: Birkhäuser Verlag, 2001 (in German).
- [2] Popovics, S. 'Calculation of the water requirement of mortar and concrete' *Materials and Structures* **13**(5)(1980)343-352.
- [3] Brouwers, H.J.H. and Radix, H.J. 'Self-compacting concrete: theoretical and experimental study' *Cem. Con. Res.* **35**(2005)2116-2136, Erratum, *ibidem* **37**(2007)1376.
- [4] Okamura, H. and Ozawa, K. 'Mix-design for Self-Compacting Concrete'. *Concrete Library, JSCE.* **25**(1995)107-120.
- [5] DAfStb - Richtlinie 'Selbstverdichtender Beton'. Berlin: Deutscher Ausschuss für Stahlbeton, Beuth Verlag, 2001 (in German).
- [6] Domone, P.L. and HsiWen, C. 'Testing of binders for high performance concrete' *Cem. Con. Res.* **27**(8)(1997)1141-1147.
- [7] Okamura, H. and Ouchi, M. 'Self-Compacting Concrete', *Journal of Advanced Concrete Technology, Japan Concrete Institute* **1**(1)(2003)5-15.
- [8] Reschke, T. *Der Einfluß der Granulometrie der Feinstoffe auf die Gefügeentwicklung und die Festigkeit von Beton*. Ph.D. Thesis, Weimar: Bauhaus University Weimar, 2000, (in German).
- [9] Marquardt, I. 'Determination of the composition of self-compacting concretes on the basis of the water requirements of the constituent materials – Presentation of a new mix concept' *Betonwerk + Fertigteiltechnik – BFT* **11**(2002)22-30.
- [10] Hunt, L.P. and Elspass, C.W. 'Particle-size properties of oilwell cements' *Cem. Con. Res.* **6**(1986)805-812.
- [11] Robens, E., Benzler, B., Büchel, G., Reichert, H. and Schumacher, K. 'Investigation of characterizing methods for the microstructure of cement' *Cem. Con. Res.* **1**(2002)87-90.
- [12] Robens, E., personal contact (2007).
- [13] Hunger, M. and Brouwers, H.J.H. 'Flow analysis of water-powder mixtures; Application to specific surface area and shape factor' *Cem. Con. Comp.* (2008) submitted.
- [14] Sympatec GmbH, 'Software algorithm for the derivation of the PSD-based specific surface area for WINDOX/HELOS-DOS 4.7 software' Clausthal-Zellerfeld, Germany (2001).